JOURNAL OF MATERIALS SCIENCE **39** (2004) 5271–5274

Nanostructured electrode materials for Ni-MH_x batteries prepared by mechanical alloying

M. JURCZYK*
Institute of Materials Science and Engineering, Poznan University of Technology, M. Sklodowska Curie 5 Sq., 60-965 Poznan, Poland
E-mail: mieczyslaw.jurczyk@put.poznan.pl

Nanocrystalline TiFe- and Mg_2Ni-type alloys were prepared by mechanical alloying followed by annealing. The structure and electrochemical properties of these materials were studied. The properties of hydrogen host materials can be modified substantially by alloying to obtain the desired storage characteristics. It was found that the respective replacement of Fe in TiFe by Ni and Mn improved not only the discharge capacity but also the cycle life of these electrodes. On the other hand, a partial substitution of Mg by Mn in $Mg_{2-x}M_xNi$ alloy leads to an increase in discharge capacity, at room temperature. Furthermore, the effect of the nickel and graphite coating on the structure of the nanocrystalline alloys and the electrodes characteristics were investigated. In Mg_2Ni-type alloy mechanical coating with graphite effectively reduced the degradation rate of the studied electrode materials.

1. Introduction

Mechanical alloying (MA) is a solid-state powder processing technique involving repeated welding, fracturing and rewelding of particles in a high-energy ball mill [1]. MA has now been shown to be capable of synthesizing a variety of equilibrium and non-equilibrium alloy phases starting from elemental powders. During MA process, the powder particles are periodically trapped between colliding balls and are plastically deformed. Such a feature occurs by the generation of a wide number of dislocations as well as other lattice defects. The non-equilibrium phases synthesized include supersaturated solid solutions, metastable crystalline and quasicrystalline phases, nanostructures and amorphous alloys. In recent years, mechanical alloying has been successfully used in the synthesis of nanocrystalline hydrogen storage materials, such as: ZrV_2, $LaNi_5$, TiFe and Mg_2Ni [2–8].

The polycrystalline TiFe(Ni) system has been widely studied in the past [9–11]. TiFe alloy, which crystallizes in the cubic CsCl-type structure, can absorb up to 2 H/f.u. at room temperature. After activation the TiFe reacts directly and reversibly with hydrogen to form two ternary hydrides TiFeH (orthorhombic) and $TiFeH_2$ (monoclinic). The discharge capacity of TiFe alloy in polycrystalline form was 0 $mA{\cdot}h{\cdot}g^{-1}$ at discharge current of 40 mA·h [12]. Magnesium-based alloys has been extensively studied during last years, as well [4, 8, 9, 13]. The polycrystalline Mg_2Ni alloy can reversibly absorb and desorb hydrogen only at high temperatures. Upon hydrogenation at 523 K, Mg_2Ni transforms into the hydride phase Mg_2NiH_4. Substantial improvements in the hydriding-dehydriding properties of TiFe and Mg_2Ni metal hydrides could possibly be achieved by formation of nanocrystalline structures [8]. It was found that the electrochemical activity of nanocrystalline hydrogen storage alloys can be improved in many ways, by alloying with other elements [2, 5], by ball-milling the alloy powders with a small amount of nickel or graphite powders [14–17]. For example, the surface modification of nanocrystalline hydrogen storage alloys with graphite by ball-milling leads to an improvement in both discharge capacity and charge-discharge cycle life [16, 17].

As a continuation of our work, in this paper, we have synthesised nanocrystalline TiFe- and Mg_2Ni-type alloys by mechanical alloying followed by annealing. The influence of manganese contents on the structural and electrochemical properties of TiFe- and Mg_2Ni-based nanocrystalline alloys were studied. Finally, the effect of the nickel and graphite coating on the structure of the alloys and the electrodes characteristics were investigated.

2. Experimental

Mechanical alloying was performed under argon atmosphere using a SPEX 8000 Mixer Mill. The purity of the starting materials was at least 99.8%. The composition of the starting powder mixture corresponded to the stoichiometry of the "ideal" reactions. In the case of Mg_2Ni-type alloys an extra 8 wt% of magnesium was used. The elemental powders (Mg: $\leq$300 μm; Ti: $\leq$45 μm; Mn: $\leq$45 μm; Fe: $\leq$10 μm; Ni: 3–7 μm) were

*Author to whom all correspondence should be addressed.

mixed and poured into the vial. The mill was run up to 20 h for TiFe-type and 90 h for Mg_2Ni-type powders preparation. The as-milled powders were heat treated at 973 K and 723 K for 0.5 h under high purity argon to form ordered TiFe- or Mg_2Ni-type phases, respectively. The powders were characterized by means of X-ray diffraction (XRD) and atomic force microscopy (AFM). XRD were performed using a X-ray powder diffractometer with Co-K_α radiation, at the various stages during milling, prior to annealing and after annealing. The crystallite sizes were estimated by using Atomic Force Microscope (AFM).

The MA and annealed powders were mixed and milled for 1 h or 30 min with 10 wt% nickel powder (3–7 μm, 99.9%) or graphite powder (45 μm, 99.999%) in a SPEX Mixer Mill, respectively. The weight ratio of hard steel balls to mixed powder was 30:1. The mechanically alloyed materials, in nanocrystalline forms, with 10 wt% addition of Ni powder, were subjected to electrochemical measurements as working electrodes. A detailed description of the electrochemical measurements was given in Refs. [4, 5].

3. Results and discussion

3.1. TiFe-type compounds

During mechanical alloying the originally sharp diffraction lines of Ti and Fe gradually become broader and their intensity decreases with milling time (not shown). The powder mixture milled for more than 20 h has transformed completely to an amorphous phase, without the formation of an other phase. The milled powder is finally heat treated to obtain the desired microstructure and properties. Formation of the nanocrystalline alloys was achieved by annealing of the amorphous material in high purity argon atmosphere at 973 K for 0.5 h. The diffraction peak was assigned to this of CsCl-type structure with cell parameter $a = 2.973$ Å (Fig. 1a). When nickel is added to $TiFe_{1-x}Ni_x$ the lattice constant a increases. The average crystallite size of the nanocrystalline TiFe powders, according to AFM studies, was of the order of 30 nm.

The discharge capacity of electrodes prepared by application of mechanically alloyed TiFe alloy powder

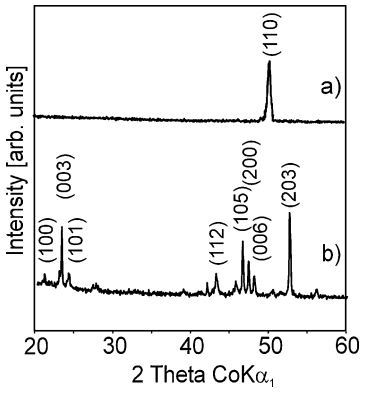

Figure 1 XRD patterns of nanocrystalline TiFe (a) and Mg_2Ni (b) alloys produced by mechanical alloying followed by annealing (TiFe MA for 20 h and heat treated at 973 K for 0.5 h; Mg_2Ni MA for 90 h and head treated at 723 K for 0.5 h).

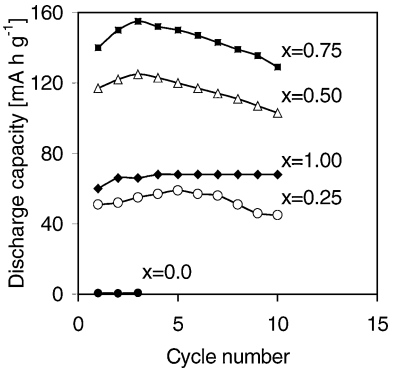

Figure 2 Discharge capacities as a function of cycle number of electrode prepared with nanocrystalline $TiFe_{1-x}Ni_x$ (solution, 6 M KOH; temperature 293 K). The charge conditions were 40 mA $\cdot$ g^{-1}. The cut-off potential vs. Hg/HgO/6 M KOH was -0.7 V.

is very low (Fig. 2). The MA TiFe alloys showed a higher discharge capacity (0.7 mA·h·g^{-1}) than the arc melted ones. The reduction of the powder size and the creation of new surfaces is effective for the improvement of the hydrogen absorption rate. Materials obtained by the substitution of Ni for Fe in $TiFe_{1-x}Ni_x$ lead to great improvement in activation behaviour of the electrodes. It was found that the increasing nickel content in $TiFe_{1-x}Ni_x$ alloys leads initially to an increase in discharge capacity, giving a maximum at $x = 0.75$ (Fig. 2). In the annealed nanocrystalline $TiFe_{0.25}Ni_{0.75}$ powder, discharge capacity of up to 155 mA·h·g^{-1} was measured. The electrodes mechanically alloyed and annealed from the elemental powders displayed the maximum capacities at around the 3-rd cycle but, especially for $x = 0.5$ and 0.75 in $TiFe_{1-x}Ni_x$ alloy, degraded slightly with cycling, This may be due to the easy formation of the oxide layer (TiO_2) during the cycling. But, the discharge capacity of nanocrystalline $TiFe_{0.125}Mn_{0.125}Ni_{0.75}$ powders has not changed much during cycling (not shown). In these nanocrystalline powders discharge capacities up to 161 mA·h·g^{-1} were measured.

In order to optimise the choice of the intermetallic compounds for a selected application, a better understanding of the role of each alloy constituent on the electronic properties of the material is crucial. Several semi-empirical models [18, 19] have been proposed for the heat of formation and heat of solution of metal hydrides and attempts have been made for justifying the maximum hydrogen absorption capacity of the metallic matrices. These models showed that the energy of the metalhydrogen interaction depend both on geometric and electronic factors. Due to the effect of disorder caused by the substitution of Fe by Ni in TiFe, the experimental valence band is broader [20]. The significant broadening of the valence band for the nanocrystalline TiFe based alloys could be explained by a strong deformation of the nanocrystals.

3.2. Mg_2Ni-type alloys

The nanocrystalline Mg_2Ni-type alloys were prepared by mechanical alloying followed by annealing. The powder mixture milled for more than 90 h has

transformed completely to the amorphous phase, without formation of another phase. Formation of the nanocrystalline alloy was achieved by annealing of the amorphous material in high purity argon atmosphere at 723 K for 0.5 h. All diffraction peaks were assigned to those of the hexagonal crystal structure with cell parameters $a = 5.216$ Å, $c = 13.246$ Å (Fig. 1b). According to AFM studies, the average size of amorphous Mg-Ni powders was of the order of 30 nm.

The unit cell volume of nanocrystalline $Mg_{1.75}Mn_{0.25}Ni$ system decreased with the increase in Mn contents. The atomic size of manganese is smaller than that of magnesium. For $x = 0.5$ in $Mg_{2-x}Mn_xNi$ the crystalline phase of a CsCl-type cubic structure is formed ($a = 3.137$ Å). The same results were obtained earlier for $(Mg_{1-x}Al_x)Ni$ system ($x = 0.2$-0.5) produced by mechanical alloying by Orimo and Fujii [4].

At room temperature, the nanocrystalline Mg_2Ni alloy absorbs hydrogen, but almost does not desorb it. At temperatures above 523 K the kinetic of the absorption-desorption process improves considerably and for nanocrystalline Mg_2Ni alloy the reaction with hydrogen is reversible. The hydrogen content in this material at 573 K is 3.25 wt%. Upon hydrogenation, Mg_2Ni transforms into the hydride Mg_2Ni-H phase. It is important to note, that between 518-483 K the hydride Mg_2Ni-H phase transforms from a high temperature cubic structure to a low temperature monoclinic phase [21]. When hydrogen is absorbed by Mg_2Ni beyond 0.3 H per formula unit, the system undergoes a structural rearrangement to the stoichiometric complex Mg_2Ni-H hydride, with an accompanying 32% increase in volume. The electrochemical properties of the alloy are improved after substitution of some amounts of magnesium by manganese. The results show that the maximum absorption capacity reaches 3.25 wt% for pure nanocrystalline Mg_2Ni alloy. This is lower than the polycrystalline Mg_2Ni alloy (3.6 wt% [9]) due to a significant amount of strain, chemical disorder and defects introduced into the material during the mechanical alloying process [8]. At the same time, increasing manganese substitution causes the unit cell to decrease. The concentration of hydrogen in produced nanocrystalline Mg_2Ni alloys strongly decreases with increasing Mn contents. The hydrogen content at 573 K in nanocrystalline $M_{1.5}Mn_{0.5}NiH$ was only 0.65 wt%.

The Mg_2Ni electrode, mechanically alloyed and annealed, displayed the maximum discharge capacity (100 mA·h·g^{-1}) at the 1st cycle but degraded strongly with cycling. The poor cyclic behaviour of Mg_2Ni electrodes is attributed to the formation of $Mg(OH)_2$ on the electrodes, which has been considered to arise from the charge-discharge cycles [22]. To avoid the surface oxidation, we have examined the effect of magnesium substitution by Mn in Mg_2Ni-type material. This alloying greatly improved the discharge capacities. In nanocrystalline $Mg_{1.5}Mn_{0.5}Ni$ alloy discharge capacities up to 241 mA·h·g^{-1} was measured. A similar phenomenon to that described here has been observed by Yuan *et al.* [23] in $Mg_{2-x}Al_xNi$-type powders.

The surface chemical composition of nanocrystalline Mg_2Ni-type alloy studied by X-ray photoelectron spectroscopy (XPS) showed the strong surface segregation under UHV conditions of Mg atoms in the MA nanocrystalline Mg_2Ni alloy. This phenomena could considerably influence the hydrogenation process in such a type of materials, as well.

3.3. Effect of ball-milling with nickel and graphite

In order to improve the electrochemical properties of the studied nanocrystalline electrode materials, the ball-milling technique was applied to the TiFe- and Mg_2Ni-type alloys using the nickel and graphite elements as a surface modifiers. The $TiFe_{0.25}Ni_{0.75}$/M- and $Mg_{1.5}Mn_{0.5}Ni$/M-type composite materials, where M = 10 wt% Ni or C, were produced by ball-milling for 1 h and 30 min, respectively. Ball-milling with nickel or graphite of $TiFe_{0.25}Ni_{0.75}$- and $Mg_{1.5}Mn_{0.5}Ni$-type materials is sufficient to considerably broaden the diffraction peaks of $TiFe_{0.25}Ni_{0.75}$ and $Mg_{1.5}Mn_{0.5}Ni$ (not shown). Additionally, milling with graphite is responsible for a sizeable reduction of the crystallite sizes of $TiFe_{0.25}Ni_{0.75}$/C and $Mg_{1.5}Mn_{0.5}Ni$/C from 30 to 20 nm.

Figs 3 and 4 show the discharge capacities as a function of the cycle number for studied nanocomposite materials. When coated with nickel, the discharge capacities of nanocrystalline $TiFe_{0.25}Ni_{0.75}$ and $Mg_{1.5}Mn_{0.5}Ni$ powders were increased. The elemental nickel was distributed on the surface of ball milled alloy particles homogenously and role of these particles is to catalyse the dissociation of molecular hydrogen on the surface of studied alloy. Mechanical coating with nickel or graphite effectively reduced the degradation rate of the studied electrode materials. Compared to that of the uncoated powders, the degradation of the coated was suppressed. Recently, Iwakura *et al.* [24] have demonstrated that the modification of graphite on the MgNi alloy in the MgNi-graphite composite is mainly a surface one. Raman and XPS investigations indicated the interaction of graphite with MgNi alloy occurred at the Mg part in the alloy. Graphite inhibits the formation of new oxide layer on the surface of materials once

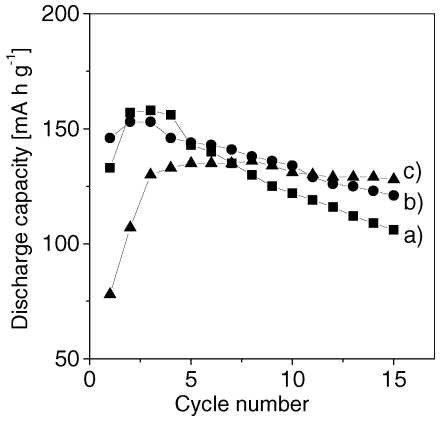

Figure 3 The discharge capacity as a function of cycle number for MA and annealed $TiFe_{0.25}Ni_{0.75}$ (a) as well as $TiFe_{0.25}Ni_{0.75}$/Ni (b) and $TiFe_{0.25}Ni_{0.75}$/C (c) composite electrodes (solution, 6 M KOH; temperature 293 K).

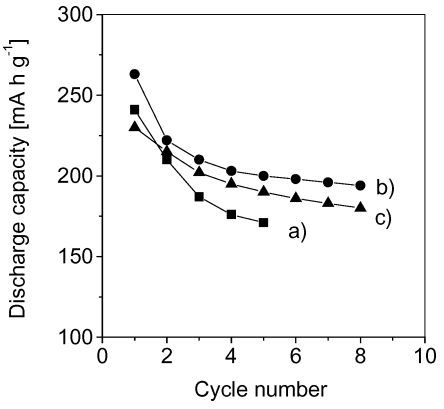

Figure 4 The discharge capacity as a function of cycle number for MA and annealed $Mg_{1.5}Mn_{0.5}Ni$ (a) as well as $Mg_{1.5}Mn_{0.5}Ni$/Ni (b) and $Mg_{1.5}Mn_{0.5}Ni$/C (c) composite electrodes (solution, 6 M KOH; temperature 293 K).

the native oxide layer is broken during the ball-milling process.

4. Conclusion

Nanocrystalline TiFe- and Mg_2Ni-type alloys synthesized by mechanical alloying and annealing were used as negative electrode materials for Ni-MH_x battery. It was found that the respective replacement of Fe in TiFe by Ni and by Mn improved not only the discharge capacity but also the cycle life of these electrodes. On the other hand, a partial substitution of Mg by Mn in $Mg_{2-x}M_xNi$ alloy leads to an increase in discharge capacity, at room temperature. It was found that milling of 10 wt% of nickel and graphite is sufficient to improve the discharge capacity of nanocomposite TiFe/M- and Mg_2Ni/M-type materials (M = Ni or C).

Acknowledgements

The financial support of the Polish National Committee for Scientific Research (KBN) under the contract No. PBZ/KBN-013/T08/02 is gratefully acknowledged (www.inmat.pw.edu.pl/nanomaterialy/). The glove box Labmaster 130 (M. Braun) was purchased by the Foundation for Polish Science under the program TECHNO–2000.

References

1. C. SURYANARAYNA, *Progr. Mater. Sci.* **46** (2001) 1.
2. A. ANANI, A. VISINTIN, K. PETROV, S. SRINIVASAN, J. J. REILLY, J. R. JOHNSON, R. B. SCHWARZ and P. B. DESCH, *J. Power Sources* **47** (1994) 261.
3. G. LIANG, J. HUOT and R. SCHULTZ, *J. Alloys Compd.* **320** (2001) 133.
4. S. I. ORIMO and H. FUJII, *Intermetallics* **6** (1998) 185.
5. M. JURCZYK, in "Research Trends. Current Topics in Electrochemistry," **9** (2003) 05.
6. M. JURCZYK, E. JANKOWSKA, M. NOWAK and J. JAKUBOWICZ, *J. Alloys Compd.* **336** (2002) 265.
7. M. JURCZYK, L. SMARDZ, K. SMARDZ, M. NOWAK and E. JANKOWSKA, *J. Solid State Chem.* **171** (2003) 30.
8. L. ZALUSKI, A. ZALUSKA and J. O. STRÖM-OLSEN, *J. Alloys Compd.* **253–254** (1997) 70.
9. G. SANDROCK, *ibid.* **293–295** (1999) 877.
10. J. J. REILLY and J. WISWALL, *Inorg. Chem.* **13** (1974) 218.
11. M. H. MINTZ, S. VAKNIN, S. BIDRMAN and Z. HADARI, *J. Appl. Phys.* **52** (1981) 463.
12. E. JANKOWSKA and M. JURCZYK, *J. Alloys Compd.* **346** (2002) L1.
13. Y. KITANO, Y. FUJIKAWA, N. SHIMIZU, S. ORIMO, H. FUJII, T. KAMINO and T. YAGUCHI, *Intermetallics* **5** (1997) 97.
14. M. AU, F. POURARIAN, S. SIMIZU, S. G. SANKAR and L. ZHANG, *J. Alloys Compd.* **223** (1995) 1.
15. D. SUN, M. LATROCHE and A. PERCHERON-GUÉGAN, *ibid.* **257** (1997) 302.
16. S. NOHARA, H. INOUE, Y. FUKUMOTO and C. IWAKURA, *ibid.* **252** (1997) L16.
17. S. BOUARICHA, J. P. DODELET, D. GUAY, J. HUOT and R. SCHULZ, *ibid.* **325** (2001) 245.
18. P. C. BOUTEN and A. R. MIEDEMA, *J. Less Common Met.* **71** (1980) 147.
19. R. GRIESSEN, *Phys. Rev.* B **38** (1988) 3690.
20. A. SZAJEK, M. JURCZYK and E. JANKOWSKA, *J. Alloys Compd.* **348** (2003) 285.
21. M. GUPTA, E. BERLIN and L. SCHALPBACH, *J. Less-Common Met.* **103** (1984) 389.
22. D. MU, Y. HATANO, T. ABE and K. WATANABE, *J. Alloys Compd.* **334** (2002) 232.
23. H. T. YUAN, L. B. WANG, R. CAO, Y. J. WANG, Y. S. ZHANG, D. Y. YAN, W. H. ZHANG and W. L. GONG, *ibid.* **309** (2000) 208.
24. C. IWAKURA, H. INOUE, S. G. ZHANG and S. NOHARA, *ibid.* **293–295** (1999) 653.

Received 11 September 2003
and accepted 27 February 2004